

# Numerical simulation of natural convection from a heated cylinder

†\*Gregor Kosec<sup>1</sup>, Jure Slak<sup>1</sup>

<sup>1</sup>Parallel and Distributed Systems Laboratory

“Jožef Stefan” Institute, Jamova 39

SI-1000 Ljubljana, Slovenia

†\*Presenting and corresponding author: gregor.kosec@ijs.si

## Abstract

In this paper, we present a meshless solution of natural convection from the heated cylinder. The numerical technique is constructed around Weighted Least Squares approximation that is used to evaluate derivatives needed to solve partial differential equations governing the problem at hand, i.e. Navier-Stokes, mass continuity, and heat transport. The results are presented in terms of temperature and velocity magnitude contour plots, as well as a more quantitative comparison with reference data in terms of Nusselt number and maximal velocity values. Three different cases are tackled, namely the standard de Vahl Davis case, natural convection from the heated cylinder, and cooling of overhead power line due to the natural convection under realistic conditions.

**Keywords:** Navier-Stokes, MLSM, de Vahl Davis, natural convection, cooling of overhead power lines.

## Introduction

Natural convection from a horizontal cylinder plays a crucial role in many heat transfer related problems ranging from heat exchangers, solar heating systems, cooling of electronic packages, to cooling of overhead power lines. One of the first studies of convective heat transfer from circular cylinders goes back to 1892 when Ayrton and Kilgour investigated the thermal emission of thin, long horizontal wires [1]. Several similar experiments followed [2], and in 1975 Morgan collected experimental data in a comprehensive review paper [3]. Based on the collected data Morgan introduced the correlations between Grashof, Prandtl and Nusselt numbers [3]. In other words, he presented relationships between the power of cooling in dependence on the material properties and the temperature difference between the cylinder and the ambient, which still serve as a basis in operative models for predicting the temperature of overhead power lines [4, 5]. There are many other similar studies where authors investigate the heat transfer from the heated cylinder due to the natural or forced convection under different conditions [2, 6, 7].

Probably the most famous article on the numerical investigation of natural convection was published in 1983 by de Vahl Davis [8], who defined and solved a reference solution for natural convection of air in a closed rectangular cavity with differentially heated vertical and isolated horizontal walls. Many researchers followed his paper and solved proposed benchmark case with different numerical techniques [9, 10], gradually establishing high confidence in the numerical solution. Similar benchmark case for the natural convection around the homogeneously heated cylinder was introduced in 1992 by Demirdžić, et al. [11], again researchers responded with different numerical solutions [12].

Although numerical methods such as the Finite Volume Method, Finite Difference Method, or the Finite Element Method are typically used for solving natural convection problems, there has been also a considerable research done in an alternative meshless solution [13-15], which appeared in the seventies with Smoothed Particles Hydrodynamics (SPH) [16]. The SPH is an answer for attacking problems, where mesh-based methods fail entirely, e.g. breaking waves, however, at the cost of inconsistency due to the combination of Eulerian kernel and Lagrangian description of motion. Nevertheless, since the introduction of SPH a myriad of different strong and weak form meshless methods appeared [17]. The conceptual difference between meshless methods and mesh-based methods is in the treatment of relations between nodes. In the mesh-based techniques the nodes need to be structured into a mesh that covers the whole computational domain, while the meshless methods do not require any special relations between nodes and can be fully defined only through the relative inter nodal positions [18]. An immediate consequence of such simplification is greater generality regarding the approximation and the position of computational points and much higher flexibility in implementation.

In this paper, we present a local meshless solution that is based on Weighted Least Squares approximation of a natural convection problem in three scenarios: the de Vahl Davis case, the Demirdžić case, and finally the cooling of overhead power line.

The rest of the paper is organized as follows. In section Governing problem the problem is introduced in section Meshless solution procedure all the details for implementation of the solution procedure are presented, in section Results, the analyses of present study are given, and in the last section, paper offers conclusions and guidelines for future work.

## Governing problem

The physical model for describing natural convection is well-established. The fluid mechanics is described with the Navier-Stokes equation, i.e. the Cauchy momentum equation with Newtonian stress tensor, and mass continuity, which is coupled with the heat transfer through the Boussinesq approximation. The model can be written nicely in the following system of partial differential equations

$$\nabla \cdot \mathbf{v} = 0, \quad (1)$$

$$\rho \frac{\partial \mathbf{v}}{\partial t} + \rho \nabla \cdot (\mathbf{v}\mathbf{v}) = -\nabla P + \nabla \cdot (\mu \nabla \mathbf{v}) + \mathbf{b}, \quad (2)$$

$$\rho \frac{\partial (c_p T)}{\partial t} + \rho \nabla \cdot (c_p T \mathbf{v}) = \nabla \cdot (\lambda \nabla T), \quad (3)$$

$$\mathbf{b} = \rho [1 - \beta_T (T - T_{\text{ref}})] \mathbf{g}, \quad (4)$$

with  $\mathbf{v}(u, v)$ ,  $P$ ,  $T$ ,  $\lambda$ ,  $c_p$ ,  $\mathbf{g}$ ,  $\rho$ ,  $\beta_T$ ,  $T_{\text{ref}}$ ,  $\mu$  and  $\mathbf{b}$  standing for velocity, pressure, temperature, thermal conductivity, specific heat, gravitational acceleration, density, the coefficient of thermal expansion, reference temperature for Boussinesq approximation, viscosity and body force, respectively. The natural convection can be characterised by two dimensionless numbers

$$\text{Ra} = \frac{|\mathbf{g}| \beta_T \Delta T \Omega^3 \rho^2 c_p}{\lambda \mu}, \quad (5)$$

$$\text{Pr} = \frac{\mu C_p}{\lambda}, \quad (6)$$

referred to as Rayleigh and Prandtl numbers, respectively, where  $\Omega$  stands for the domain dimension.

We will consider three cases. First, the de Vahl Davis case to confirm the solution procedure, second, the heated cylinder case to demonstrate the flexibility of meshless method regarding the geometry, and finally a cooling of the overhead power line by natural convection under realistic conditions. The cases differ in geometry, boundary conditions and thermo-physical properties. The de Vahl Davis case is the most straightforward, since the closed square cavity with impermeable no-slip velocity boundary conditions, differentially heated vertical, and isolated horizontal walls are considered. The heated cylinder case is a bit more challenging due to the irregular geometry introduced by a cylinder in the domain. The last case, the cooling of the overhead power line is the most challenging due to realistic conditions and presence of velocity Neumann boundary conditions. All three cases are presented in Figure 1.

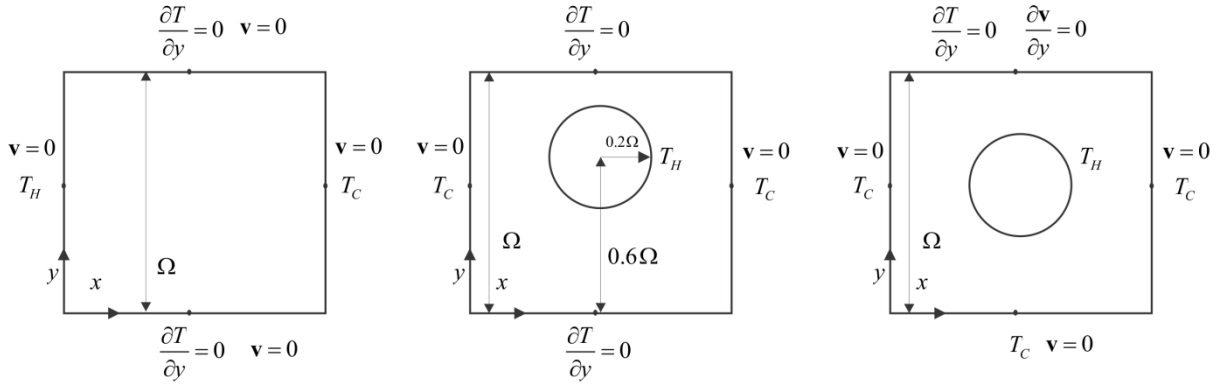


**Figure 1: Geometry and boundary conditions for de Vahl Davis case (left), Demirdžić case (middle), and cooling of the overhead power line (right).**

## Meshless solution procedure

### *Spatial discretization*

Spatial discretization is based on a local approximation of a considered field over the overlapping local support domains, i.e. in each node an approximation over a small local subset of neighbouring  $n$  nodes among all nodes  $N$

$$\hat{u}(\mathbf{p}) = \sum_i^m \alpha_i b_i(\mathbf{p}) = \mathbf{b}(\mathbf{p})^T \boldsymbol{\alpha}, \quad (7)$$

with  $m$ ,  $\boldsymbol{\alpha}$ ,  $\mathbf{b}$ ,  $\mathbf{p}(p_x, p_y)$  standing for the number of basis functions, approximation coefficients, basis functions and the position vector, respectively, is used. Using the same number of basis functions as a number of support domain, i.e.  $n = m$ , the determination of coefficients  $\boldsymbol{\alpha}$  simplifies to solving a system of  $n$  linear equations that result from expressing eq. (7) in each support node.

$$u(\mathbf{p}_j) = \mathbf{u} = \mathbf{b}(\mathbf{p})^T \boldsymbol{\alpha}, \quad (8)$$

$\mathbf{p}_j$  are positions of support nodes and  $\mathbf{u}$  are values of the considered field in the support positions. The above system can be written in a matrix form as

$$\mathbf{u} = \mathbf{B}\boldsymbol{\alpha}, \quad (9)$$

where  $\mathbf{B}$  stands for a coefficient matrix with elements  $B_{ji} = b_i(\mathbf{p}_j)$ . Using a higher number of support nodes than the number of basis functions, i.e.  $n > m$ , a Weighted Least Squares (WLS) approximation is used to solve the over-determined problem. In other words a norm

$$r^2 = \sum_j^n W(\mathbf{p}_j) (u(\mathbf{p}_j) - \hat{u}(\mathbf{p}_j))^2 = (\mathbf{B}\boldsymbol{\alpha} - \mathbf{u})^T \mathbf{W}(\mathbf{B}\boldsymbol{\alpha} - \mathbf{u}), \quad (10)$$

is minimized, where  $\mathbf{W}$  is a diagonal matrix with elements  $W_{jj} = W(\mathbf{p}_j)$  with

$$W(\mathbf{p}) = \exp\left(-\left(\frac{\|\mathbf{p}_0 - \mathbf{p}\|}{\sigma p_{\min}}\right)^2\right), \quad (11)$$

where  $\sigma$  stands for weight parameter,  $\mathbf{p}_0$  for the centre of support domain and  $p_{\min}$  for the distance to the first support domain node. The solution can be written in matrix form as

$$\boldsymbol{\alpha} = (\mathbf{W}^{0.5}\mathbf{B})^+ \mathbf{W}^{0.5}\mathbf{u}, \quad (12)$$

where  $(\mathbf{W}^{0.5}\mathbf{B})^+$  stand for a Moore–Penrose pseudo inverse. By explicit expression of  $\boldsymbol{\alpha}$  into (8) an equation

$$\hat{u}(\mathbf{p}) = \mathbf{b}(\mathbf{p})^T (\mathbf{W}^{0.5}(\mathbf{p})\mathbf{B})^+ \mathbf{W}^{0.5}(\mathbf{p})\mathbf{u} = \boldsymbol{\chi}(\mathbf{p})\mathbf{u}, \quad (13)$$

is obtained, where  $\boldsymbol{\chi}$  stand for the shape function. Now, we can apply partial differential operator, which is our goal, on the trial function,

$$L\hat{u}(\mathbf{p}) = L\boldsymbol{\chi}(\mathbf{p})\mathbf{u}, \quad (14)$$

where  $L$  stands for a general differential operator. In this paper, we deal with a Navier-Stokes equation and therefore only shape functions for Laplace operator and first derivatives are needed, which are pre-computed and stored

$$\boldsymbol{\chi}^{\hat{x}}(\mathbf{p}) = \frac{\partial}{\partial x} \mathbf{b}(\mathbf{p})^T (\mathbf{W}^{0.5}(\mathbf{p})\mathbf{B})^+ \mathbf{W}^{0.5}, \quad (15)$$

$$\boldsymbol{\chi}^{\hat{y}}(\mathbf{p}) = \frac{\partial}{\partial y} \mathbf{b}(\mathbf{p})^T (\mathbf{W}^{0.5}(\mathbf{p})\mathbf{B})^+ \mathbf{W}^{0.5}, \quad (16)$$

$$\boldsymbol{\chi}^{\nabla^2}(\mathbf{p}) = \nabla^2 \mathbf{b}(\mathbf{p})^T (\mathbf{W}^{0.5}(\mathbf{p})\mathbf{B})^+ \mathbf{W}^{0.5}, \quad (17)$$

The presented formulation is convenient for implementation since most of the complex operations, i.e. finding support nodes and building shape functions, are performed only when nodal topology changes. In the main simulation, the pre-computed shape functions are then convoluted with the vector of field values in the support to evaluate the desired operator. We will refer to this approach as to the Meshless Local Strong Form Method (MLSM) in further discussions.

#### *Positioning of computational nodes*

The presented MLSM approach can be understood as a generalisation of FDM. Despite its simplicity it offers many possibilities for treating challenging cases, e.g. nodal adaptivity to address regions with sharp discontinuities or p-adaptivity to treat obscure anomalies in

physical field. Furthermore, the stability versus computation complexity and accuracy can be regulated merely by changing a number of support nodes, etc. In this paper, we will exploit the generality to solve the problem in an irregular domain. Although the above formulation does not need an exact mesh, it is expected that using regularly distributed nodes lead to more accurate and stable results [18-20]. Therefore, despite seeming robustness of meshless methods regarding the nodal distribution, a certain effort has to be invested into the positioning of the nodes [21], with the ultimate goal to maximize stability and accuracy and retain the generality of the meshless principle. A possible approach to achieve that is to distribute nodes with a straightforward algorithm based on Poisson Disk Sampling. Such algorithms have been already used in a meshless context [22] and will also be used here. The general idea is to put a seed node randomly within the domain. Then, add new nodes on a circle with centre in the seed node and radius supplied as a desired nodal density parameter  $\delta r$  where the value of  $\delta r$  represents the desired distance between nodes. In the next iteration one of the newly added nodes is selected as the new seed node and the procedure repeats. Example of nodes positioned within the domain that will be tackled in numerical examples with the Poisson Disk Sampling algorithm is depicted in Figure 2.

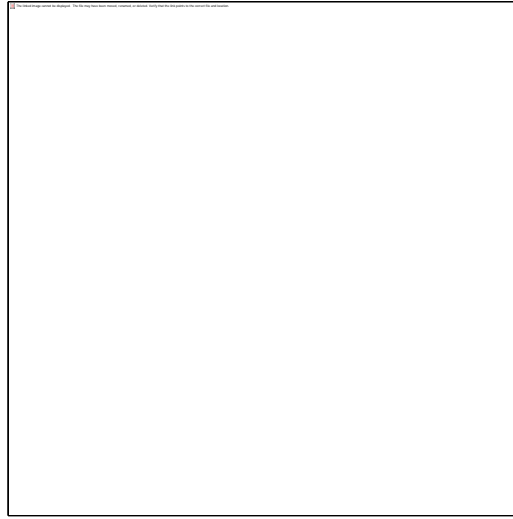


**Figure 2: Nodes positioned with a Poisson Disk Sampling algorithm.**

### *Solution procedure*

Each time step begins with computing new intermediate velocity from the equation (2) without pressure term with explicit Euler's method. Since the intermediate velocity does not satisfy equation (1), a Poisson pressure correction equation

$$\nabla^2 p^{corr} = \frac{\rho}{\Delta t} \nabla \cdot \mathbf{v}^{iter} , \quad (18)$$

where  $\Delta t$  stand for time step and  $\mathbf{v}^{iter}$  for intermediate velocity, is solved with following boundary condition

$$\frac{\Delta t}{\rho} \frac{\partial p^{corr}}{\partial n} = \hat{\mathbf{n}} \cdot (\mathbf{v}^{iter} - \mathbf{v}^{BC}) , \quad (19)$$

where  $\hat{\mathbf{n}}$  stands for the outside unit normal vector. The pressure Poisson equation is, at given boundary conditions, defined only up to a constant and to avoid instabilities a unique solution is enforced with an additional condition, also referred to as a regularization

$$\int_{\Omega} p d\Omega = 0. \quad (20)$$

Once the pressure correction is known, a velocity is corrected accordingly

$$\mathbf{v}^{corr} = -\frac{\Delta t}{\rho} \nabla P^{corr}. \quad (21)$$

Finally, the equation (3) is solved, again with Euler method.

## Results

### *De Vahl Davis benchmark case*

De Vahl Davis investigated natural convection of air with  $Pr = 0.71$  up to  $Ra = 10^6$  in his original paper. However, more intense solutions followed with the most volatile case of  $Ra = 10^8$ . Here, we focus only on the  $Ra = 10^8$  case. Results are presented in terms of temperature and velocity magnitude contour plots in Figure 3. A more quantitative result is shown in Figure 4, where a hot side Nusselt number and maximal vertical cross-section velocity with respect to the number of nodes used are compared against reference solutions [23] (a), [9] (b) and [10] (c). It can be clearly seen that the solutions of MLSM approach converge towards values that are within the dispersion of the reference solutions and we can conclude that the presented solution procedure can handle intense natural convection cases on regular nodal distributions.

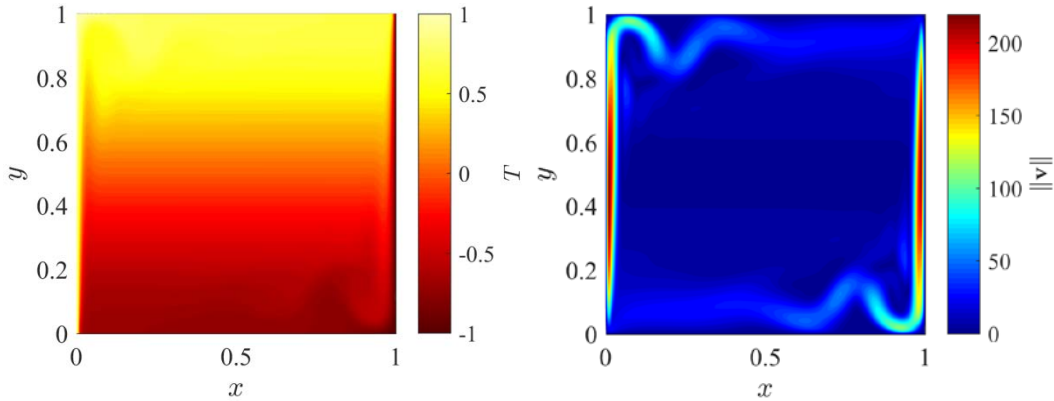


**Figure 3: Temperature (left) and velocity magnitude (right) contour plots for de Vahl Davis case at  $Ra = 10^8$ .**

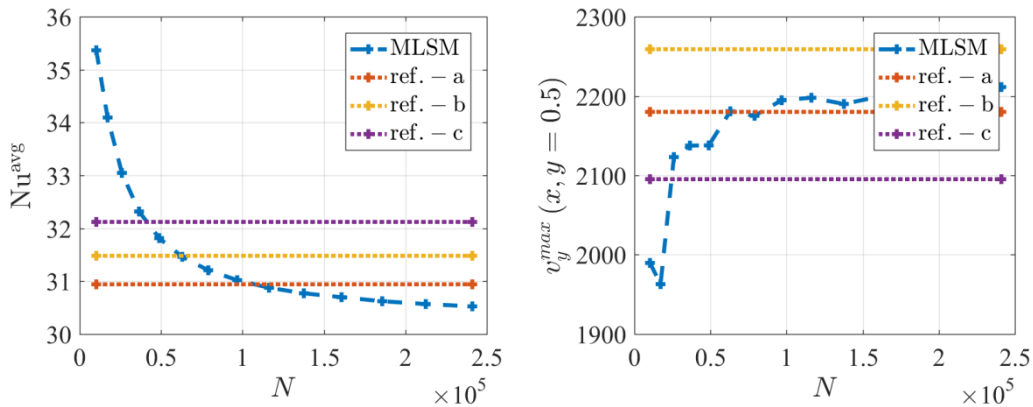


**Figure 4: Average hot side Nusselt number (left) and maximal vertical velocity (right) with respect to the number of used nodes  $N$  for  $Ra = 10^8$  case.**

### Heated cylinder case benchmark case

In a next case, the natural convection from a cylinder whose wall is maintained at a constant temperature  $T_H$ , enclosed by a square duct with vertical walls kept at constant temperature, and horizontal walls assumed adiabatic, is considered. The cylinder centre is displaced from the duct centre vertically for 10%, and its radius is 20% of domain height. The temperature and velocity magnitude contour plots computed by MLSM approach are presented in Figure 5. Furthermore, in Figure 6 MLSM solution is compared against reference data [11] in terms of isotherms and cold side Nusselt number. We can observe that the MLSM solution agrees well with the data provided by Demirdžić, et al.

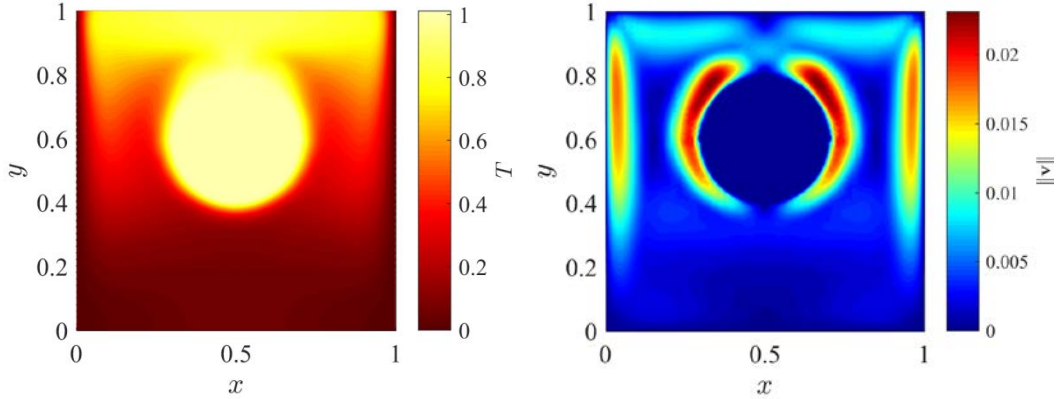


**Figure 5: Temperature (left) and velocity magnitude (right) contour plots for Demirdžić case.**

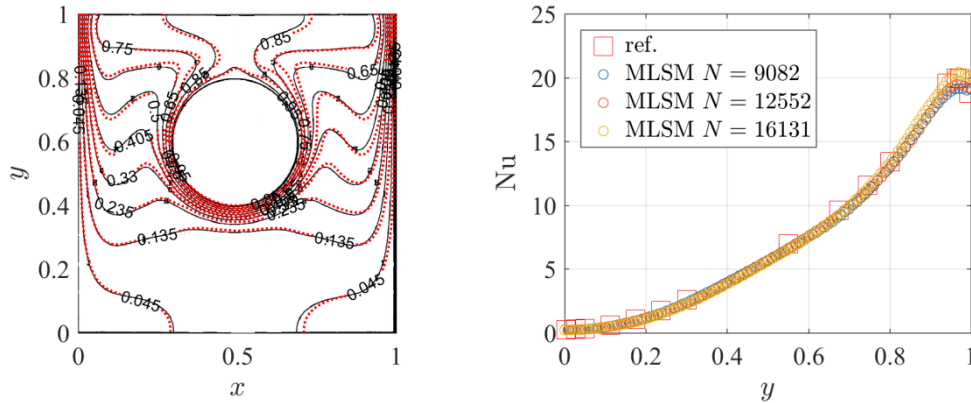


**Figure 6: Comparison between MLSM solution and data from [11] in terms of isotherms (left) and cold side Nusselt number (right).**

### Cooling of overhead power line case

In the last numerical example, we examine a cooling of the overhead power line by natural convection. The problem is very similar to the previous one, with the main difference in a top boundary condition, where instead of confined cavity an open domain is assumed. Besides, the thermo-physical properties of real materials are considered and not dimensionless characterisation as in previous two examples. The power line 490-AL1/64-ST1A with radius 1.33 cm is positioned in the centre of in 5x5 cm square domain, and the air is modelled with following properties:  $\rho = 1.29 \text{ kg/m}^3$ ,  $c_p = 1005 \text{ J/kgK}$ ,  $\beta = 0.00367$ , thermal conductivity modelled as

$$\lambda_a = 2.368 \cdot 10^{-2} + 7.23 \cdot 10^{-5} T - 2.763 \cdot 10^{-8} T^2 \left[ \frac{\text{W}}{\text{mK}} \right], \quad (22)$$

and viscosity modelled as

$$\mu = (17.239 + 4.635 \cdot 10^{-2} T - 2.03 \cdot 10^{-5} T^2) \cdot 10^{-6} [\text{Pa s}]. \quad (23)$$

First, the temperature and velocity magnitude contour plots for  $T_C = 0^\circ \text{C}$   $T_H = 80^\circ \text{C}$  are presented in Figure 7. In a next analysis (Figure 8) we compare the power of convective cooling computed by presented MLSM solution procedure against two leading standards, namely CIGRE [4] and IEEE [5]. Although the agreement is not perfect, we are satisfied with the results. It is essential to understand that CIGRE and IEEE computations rely only on empirical relations, while the MLSM solution uses solely physical model and thermo-physical properties of air.

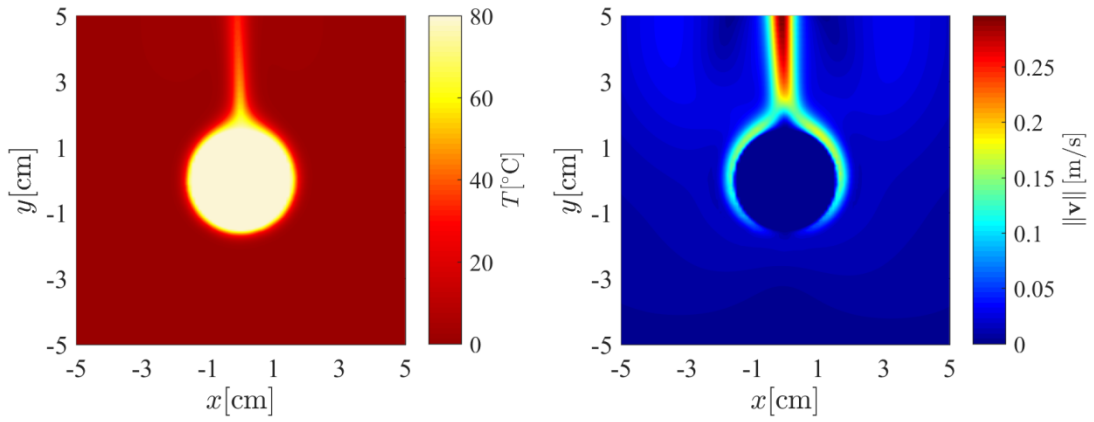


**Figure 7: Temperature (left) and velocity magnitude (right) contour plots for cooling of overhead power line case at skin temperature  $80^\circ \text{C}$ .**

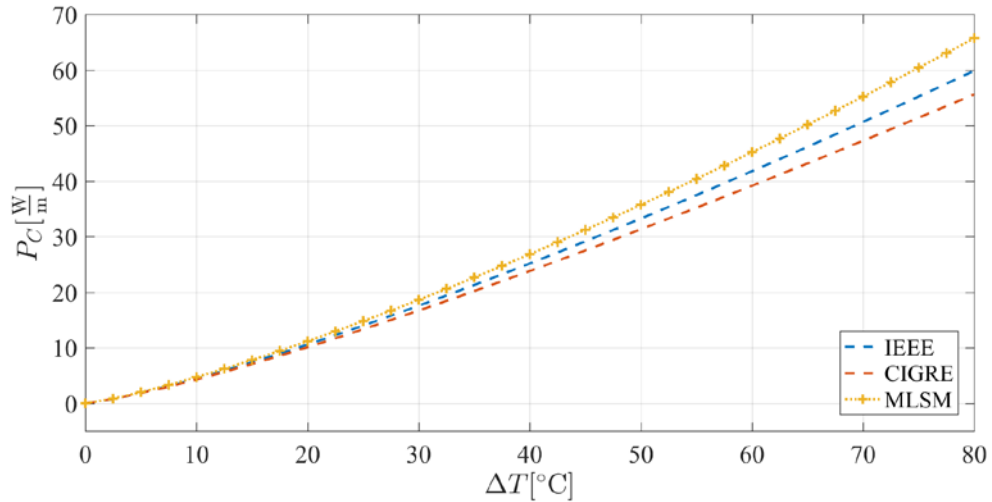


**Figure 8: Power of convective cooling with respect to the difference between the skin temperature and ambient temperature ( $\Delta T = T_H - T_C$ ).**

## Conclusions

In this paper, we demonstrated the usability of the meshless method in solving the natural convection from a heated cylinder. First, we established some confidence in the solution procedure by solving the standard de Vahl Davis case on the regular nodal distributions. Next, we attacked a bit more complicated case of natural convection in the irregular domain. As for the last numerical example, we demonstrated the simulation of cooling of the overhead power line by natural convection.

In all presented cases the results computed with MLSM are in good agreement with the reference data. In the future work we would like to present also a coordinate free implementation of MLSM and compare its performance with more established numerical libraries.

## References

- [1] Ayrton, W. & Kilgour, H., The thermal emissivity of thin wires in air. . *Philos TR Soc A*, **183**, pp. 371–405, 1892.
- [2] Boetcher, S. K. S., *Natural Convection from Circular Cylinders*, Springer: Daytona Beach, 2014.
- [3] Morgan, V., The overall convective heat transfer from smooth circular cylinders. *Advances in Heat Transfer*, **1**, pp. 199-264, 1975.
- [4] Guide for Thermal Rating Calculations of Overhead Lines. pp. 2014.
- [5] IEEE Standard for Calculating the Current-Temperature Relationship of Bare Overhead Conductors. pp. 2014.
- [6] Atmane, Mohamed A., Chan, Victor S.S. & Murray, Darina B., Natural convection around a horizontal heated cylinder: The effects of vertical confinement. *International Journal of Heat and Mass Transfer*, **46**, pp. 3661-3672, 2003.
- [7] Cesinia, G. , Paroncinia, M. , Cortellab G. & Manzanb, M., Natural convection from a horizontal cylinder in a rectangular cavity. *International Journal of Heat and Mass Transfer*, **42**, pp. 1801-1811, 1999.
- [8] de Vahl Davis, G., Natural convection of air in a square cavity: a bench mark numerical solution. *International Journal for Numerical Methods in Fluids*, **3**, pp. 249-264, 1983.
- [9] Wan, D. C., Patnaik, B. S. V. & Wei, G. W., A new benchmark quality solution for the buoyancy-driven cavity by discrete singular convolution. *Numerical Heat Transfer*, **B40**, pp. 199-228, 2001.
- [10] Kosec, G. & Šarler, B., Solution of thermo-fluid problems by collocation with local pressure correction. *International Journal of Numerical Methods for Heat & Fluid Flow*, **18**, pp. 868-882, 2008.
- [11] Demirdžić, I., Lilek, Ž & Perić, M., Fluid flow and heat transfer test problems for non-orthogonal grids: Bench-mark solutions. *International Journal for Numerical Methods in Fluids*, **15**, pp. 329–354, 1992.
- [12] Roychowdhury, D. G., Das, Sarit K. & Sundararajan, T., Numerical simulation of natural convective heat transfer and fluid flow around a heated cylinder inside an enclosure. *Heat and Mass Transfer*, **38**, pp. 565-576, 2002.
- [13] Kosec, G., Depolli, M., Rashkovska, A. & Trobec, R., Super linear speedup in a local parallel meshless solution of thermo-fluid problems. *Computers & Structures*, **133**, pp. 30-38, 2014.
- [14] Arefmanesh, A., Najafi, M. & Musavi, S. H., Buoyancy-driven fluid flow and heat transfer in a square cavity with a wavy baffle—Meshless numerical analysis. *Engineering Analysis with Boundary Elements*, **37**, pp. 366–382 2013.
- [15] Wang, C. A., Sadat, H. & Prax, C., A new meshless approach for three dimensional fluid flow and related heat transfer problems. *Computers and Fluids*, **69**, pp. 136-146, 2012.
- [16] Gingold, R. A. & Monaghan, J. J., Smoothed particle hydrodynamics: theory and application to non-spherical stars. *Mon. Not. Roy. Astron. So*, **181**, pp. 375-389, 1977.
- [17] Nguyen, V. P. , Rabczuk, T., Bordas, S. & Duflot, M., Meshless methods: a review and computer implementation aspects. *Mathematics and computers in simulation*, **79**, pp. 763--813, 2008.
- [18] Trobec, R & Kosec, G., *Parallel scientific computing : theory, algorithms, and applications of mesh based and meshless methods*, Springer: 2015.
- [19] Trobec, R., Kosec, G., Šterk, M. & Šarler, B., Comparison of local weak and strong form meshless methods for 2-D diffusion equation. *Engineering Analysis with Boundary Elements*, **36**, pp. 310-321, 2012.

- [20] Amani, J., Afshar, M.H. & Naisipour, M., Mixed discrete least squares meshless method for planar elasticity problems using regular and irregular nodal distributions. *Engineering Analysis with Boundary Elements*, **36**, pp. 894-902, 2012.
- [21] Kosec, G., A local numerical solution of a fluid-flow problem on an irregular domain. *Advances in Engineering Software*, **120**, pp. 36-44, 2018.
- [22] Fornberg, B. & Flyer, N., Fast generation of 2-D node distributions for mesh-free PDE discretizations. *Computers Mathematics with Applications*, **69**, pp. 2015.
- [23] Sadat, H. & Couturier, S., Performance and accuracy of a meshless method for laminar natural convection. *Numerical Heat Transfer*, **B37**, pp. 455-467, 2000.